Bernadette Hammer-Rotzler, Jörg Neuhausen, Christof Vockenhuber, Viktor Boutellier, Michael Wohlmuther, Andreas Türler, and Dorothea Schumann*

Radiochemical determination of ^{129}I and ^{36}Cl in MEGAPIE, a proton irradiated lead-bismuth eutectic spallation target

DOI 10.1515/ract-2015-2420
Received April 1, 2015; accepted July 17, 2015; published online September 14, 2015

Abstract: The concentrations of the long-lived nuclear reaction products ^{129}I and ^{36}Cl have been measured in samples from the MEGAPIE liquid metal spallation target. Samples from the bulk target material (lead-bismuth eutectic, LBE), from the interface of the metal free surface with the cover gas, from LBE/steel interfaces and from noble metal absorber foils installed in the cover gas system were analysed using Accelerator Mass Spectrometry at the Laboratory of Ion beam Physics at ETH Zürich. The major part of ^{129}I and ^{36}Cl was found accumulated on the interfaces, particularly at the interface of LBE and the steel walls of the target container, while bulk LBE samples contain only a minor fraction of these nuclides. Both nuclides were also detected on the absorber foils to a certain extent ($\ll$ 1% of the total amount). The latter number is negligible concerning the radio-hazard of the irradiated target material; however it indicates a certain affinity of the absorber foils for halogens, thus proving the principle of using noble metal foils for catching these volatile radionuclides. The total amounts of ^{129}I and ^{36}Cl in the target were estimated from the analytical data by averaging within the different groups of samples and summing up these averages over the total target. This estimation could account for about half of the amount of ^{129}I and ^{36}Cl predicted to be produced using nuclear physics modelling codes for both nuclides. The significance of the results and the associated uncertainties are discussed.

***Corresponding author: Dorothea Schumann,** Paul Scherrer Institute, 5232 Villigen PSI, Switzerland, e-mail: dorothea.schumann@psi.ch
Bernadette Hammer-Rotzler, Andreas Türler: Paul Scherrer Institute, 5232 Villigen PSI, Switzerland; and University of Bern, 3012 Bern, Switzerland
Jörg Neuhausen, Viktor Boutellier, Michael Wohlmuther: Paul Scherrer Institute, 5232 Villigen PSI, Switzerland
Christof Vockenhuber: Laboratory of Ion Beam Physics, ETH Zurich, 8093 Zurich, Switzerland

Keywords: Liquid metal chemistry, lead-bismuth-eutectic, radiochemical separation, accelerator mass spectrometry.

1 Introduction

Accelerator-Driven Systems (ADS) are one of the promising options in GenIV reactor concepts, because they cover both the energy production on a largely improved safety level and the transmutation of already existing long-lived nuclear waste into short-lived or stable isotopes. An ADS consists of an accelerator, a spallation target and a subcritical reactor core [1, 2]. Liquid lead-bismuth eutectic (LBE) is a possible target and coolant material due to its favourable nuclear, thermophysical and chemical properties [3, 4]. In the target, radioactive and stable nuclides with masses up to one mass unit higher than the mass of the target components are generated by different proton induced nuclear reactions like for instance spallation and fission. From a safety point of view, special attention has to be paid to the behaviour of radioactive isotopes of volatile elements like Hg, Cl or I. In the case of LBE, the α-emitters $^{208-210}$Po generated from bismuth imply an additional risk due to the radiotoxicity of these nuclides combined with the significant volatility of the element polonium.

A prototype of a liquid metal spallation target – MEGAPIE (MEGAWatt PIlot Experiment) [5] – was tested in the spallation source SINQ at PSI in 2006, being the first liquid spallation target close to the megawatt range using lead-bismuth eutectic (LBE). The aim of the project was to design, build, operate and explore a liquid LBE spallation target of 1 MW beam power [6]. This first test experiment has been a milestone in the roadmap towards the demonstration of a working ADS concept and the feasibility of high power liquid metal targets in general [7].

For a safe operation of such a facility, the knowledge of the residual nuclide production in the target as well as the activation of the surrounding components is mandatory. Furthermore, the chemical behaviour of the generated radionuclides determining their distribution in the system is certainly safety relevant. Consequently, radiochemical

analyses of irradiated materials from liquid metal targets to determine both the content and distribution of generated radionuclides are important to benchmark theoretical predictions of nuclide production as well as for the estimation of safety hazards of future lbe nuclear facilities during and after operation, the latter also including options for intermediate or final disposal. The analysis of samples from the irradiated MEGAPIE target, within its post-irradiation examination (PIE) program [8], is a unique opportunity to collect such data on radionuclide production and distribution within a high power liquid metal spallation target.

Among the many radionuclides produced in a liquid LBE spallation target, those of the halogens chlorine and iodine are of special interest because these elements are volatile and many of their isotopes show decay characteristics that make them problematic concerning safety: iodine has several short-lived isotopes (^{123}I, ^{124}I, ^{125}I, ^{126}I, ^{130}I, ^{131}I, ^{132}I, ^{133}I, ^{135}I) that may cause radiological problems when released during operation. On the other hand, the long-lived ^{129}I ($T_{1/2} = 1.57 \times 10^7$ y) – mainly a high-energetic fission product – and ^{36}Cl ($T_{1/2} = 3.01 \times 10^5$ y) – produced by fragmentation as well as neutron activation from Cl impurities, are important for the final disposal of the irradiated target material.

In this paper, we report on analytical results for the ^{129}I and ^{36}Cl content in the megapie target, obtained using accelerator mass spectrometry (AMS) after a radiochemical separation of the elements from samples representing different locations within the MEGAPIE target, specifically the bulk target material, its interfaces with the construction materials (steel) and the cover gas, and a set of noble metal foils that were installed in the cover gas volume to capture released volatile radionuclides. We discuss the inhomogeneous distribution of the nuclides found within the target and outline a method to roughly estimate the total ^{129}I and ^{36}Cl content of the target from the analytical data. Finally, we compare the obtained results to theoretical predictions of the production of the nuclides under investigation obtained by nuclear physics codes and discuss uncertainties and practical consequences.

2 The MEGAPIE target

2.1 Irradiation

The MEGAPIE target was irradiated for 123 days, starting in mid-August 2006, with an averaged current of 0.947 mA of 575 MeV protons [9]. The LBE exposed to the proton beam was continually pumped through the target system (Figure 1) with a flowrate of 4 L/s, corresponding to velocities of 0.2 to 1.2 m/s in different zones and components [10]. At the beam entry with the highest proton density the LBE was heated by the proton beam to about 340 °C to 350 °C [11, 12]. From this nuclear reaction zone, the liquid metal moved upwards through the electromagnetic pump until it was diverted close to the top of the target (segment H07) to flow down again through the heat exchanger, where it was cooled down to approx. 230 °C [11] and finally returned to the nuclear reaction zone. In the topmost part of the target, the LBE loop was connected to an expansion volume, where the liquid metal was in contact with a cover gas (Ar). The mass transfer between the loop and this expansion volume was enhanced by level changes of the liquid metal caused by thermal expansion and contraction of the LBE with changing operating conditions (temperature changes induced by beam trips and switching between standby and full power operation modes). In the gas space of the expansion volume, a set of noble metal foils (Ag and Pd) was installed to serve as adsorber for volatile radionuclides potentially released to the gas phase. This expansion volume was connected to a large and complex cover gas system [10] that served for storing gases until their radioactivity decreased sufficiently to allow venting.

The nuclear reaction products – mainly formed in the beam entrance zone – were circulated through the target system by the liquid metal flow, being exposed to thermal gradients and coming in contact with surfaces of the structural materials. In this complex system, the nuclear reaction products can undergo numerous chemical reactions with the target material itself, other nuclear reaction products in LBE, the structural materials and impurities in the target material and the cover gas [13, 14]. These reactions may cause formation of compounds insoluble in the liquid metal or volatile species that are released from the liquid metal, thus leading to inhomogeneous distribution. The consequences of this scenario for the analysis of samples from the MEGAPIE target and interpretation of the obtained data are discussed in the following sections.

2.2 Radiological and chemical boundary conditions

The nature of the MEGAPIE target makes it a challenging object for chemical analysis because of various reasons. The target is highly radioactive after its irradiation, making sample taking a tremendously difficult task involving a lot of complex, time consuming and expensive hot-cell work. Moreover, the target itself is an extremely complex system where the liquid metal not only serves as spalla-

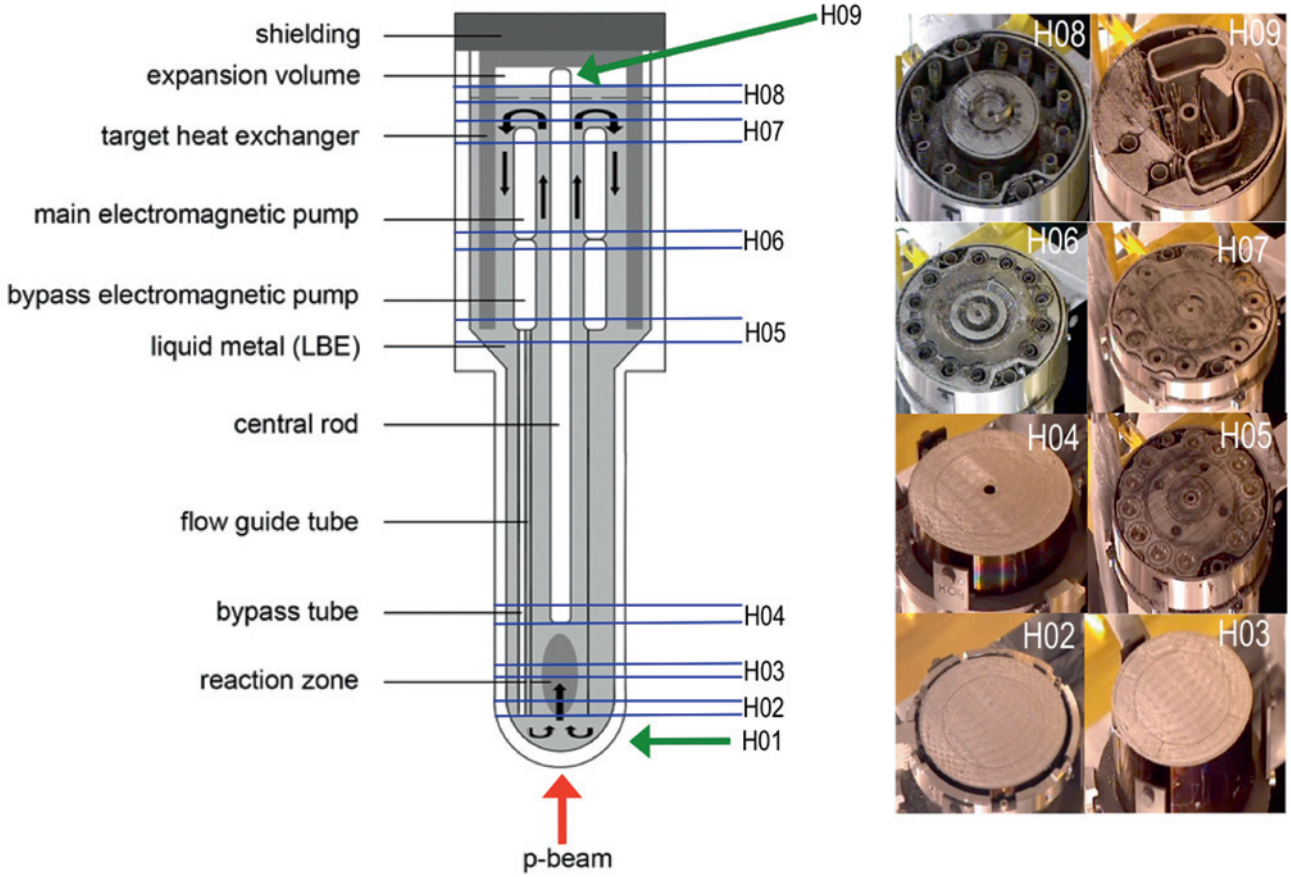

Fig. 1: Scheme of the MEGAPIE target assembly and its main components. The liquid metal flow is indicated by the black arrows in the inner part of the scheme. The locations of the segments used for the post-irradiation examination are indicated by horizontal lines. Photographs of the segments after cutting are shown on the right hand side.

tion target but also as a medium for chemical reactions involving the generated radionuclides. The liquid metal and the radionuclides therein are exposed to a complex flow field and temperature gradients, where the contact with construction materials and the cover gas – including impurities contained therein – may lead to chemical reactions causing inhomogeneous distribution of the nuclides [13, 14]. In particular, accumulation of insoluble materials may occur on surfaces, as was reported for nuclides of electropositive elements such as ^{173}Lu [15]. A further complication arises from the possible release of volatile elements from the liquid metal to the cover gas system that can potentially lead to depletion in the target material.

This complexity makes it desirable to analyse sets of samples from as many different locations within the target as possible. However, the analysis of ^{129}I and ^{36}Cl requires a relatively complex analytical procedure involving chemical separations followed by Accelerator Mass Spectrometry (AMS), limiting the number of samples that could be analysed with reasonable effort. We therefore strived for a compromise between the demand for representative sampling and the practical limitations posed by radioprotection issues and availability of AMS by analysing a reasonable number of samples from different locations within the target, i.e. the bulk LBE, its contact interfaces with the construction materials and the cover gas and also samples from the noble metal foils installed in the cover gas for capturing volatile elements. Based on the distribution of the studied radionuclides, we calculated values for the individual types of samples that can be used to roughly estimate the total content, which then can be compared to the results of predictions obtained by nuclear physics codes. The uncertainties of this approach will be critically discussed.

2.3 Sampling procedure

After a decay period from 2006 to 2009, the target was cut into the segments H01 up to H09 (Figure 1). Samples were taken from segments H02 to H09, from the lower part H02 to H06 by core drilling either in the bulk LBE or at the

Table 1: Overview of all analysed samples and details of their characteristics.

	m [mg]	Type	Material	LBE flow	Analysed nuclides
H02-U2	11.8	bulk	LBE	up flow	^{129}I
	15.4				
H03-U12	19.6	bulk	LBE	up flow	^{36}Cl, ^{129}I
H04-U	15.7	bulk	LBE	up flow	^{36}Cl, ^{129}I
H05-U	12.7	bulk	LBE	up flow	^{36}Cl, ^{129}I
H06-U-b	21.1	bulk	LBE	up flow	^{129}I
H07-S-b	11.3	bulk	LBE	up flow	^{36}Cl, ^{129}I
H07-D-b	28.4	bulk	LBE	down flow	^{36}Cl, ^{129}I
H06-S	31.5	bulk	LBE	down flow	^{36}Cl, ^{129}I
H04-B	12.7	bulk	LBE	down flow	^{36}Cl, ^{129}I
H03-D2	31.9	bulk	LBE	down flow	^{129}I
H02-D2	8.4	bulk	LBE	down flow	^{36}Cl, ^{129}I
H07-S	10.3	LBE/cover gas-interface	LBE		^{36}Cl, ^{129}I
H07-U2	14.7	free surface	LBE		^{36}Cl, ^{129}I
H08-U1-b	12.0	free surface	LBE		^{36}Cl, ^{129}I
H08-U2	14.2	free surface	LBE		^{36}Cl, ^{129}I
	16.4				
H03-U6	9	LBE/steel-interface	LBE	up flow	^{36}Cl, ^{129}I
H05-U4-b	0.212	LBE/steel-interface	steel	up flow	^{36}Cl, ^{129}I
H06-D2S	10.9	LBE/steel-interface	LBE	down flow	^{36}Cl, ^{129}I
	6.9				
	0.095		steel	down flow	^{36}Cl, ^{129}I
	0.092				
H05-D62-b	17	LBE/steel-interface	LBE	down flow	^{36}Cl, ^{129}I
H05-D6-b					
	0.058		steel	down flow	^{36}Cl, ^{129}I
H05-D22	15.6(a)	LBE/steel-interface	LBE	down flow	^{129}I
	8.4(b)				
H03-D4	10.3	LBE/steel-interface	LBE	down flow	^{129}I
absorber 1	28.9	absorber foil	Ag		^{36}Cl, ^{129}I
	27.5				
absorber 2	13.4	absorber foil	Ag		^{36}Cl, ^{129}I
	28.0				
absorber 3	10.6	absorber foil	Ag		^{36}Cl, ^{129}I
	45.6				
absorber 4	14.6	absorber foil	Ag		^{36}Cl, ^{129}I
	25.2				
absorber 5	23.3	absorber foil	Ag		^{36}Cl, ^{129}I
	30.1				
absorber 6	17.3	absorber foil	Pd		^{36}Cl, ^{129}I
	6.8				
	4.8				
absorber 7	24.7	absorber foil	Ag		^{36}Cl, ^{129}I
	21.6				

interface with the steel, from section H08 by breaking or scratching off material sticking to the walls. From section H07, both core drillings from the free surface as well as material sticking to the wall were retrieved. The stack of noble metal absorber foils located in H09 was removed completely and small pieces of the individual foils were cut.

From the 75 samples obtained in this way, a set was selected for the analysis of ^{36}Cl and ^{129}I that represents different locations in the MEGAPIE target, H03 up to H08 and the absorber foils in the expansion volume located in H09, comprising various samples from the bulk LBE, the LBE/steel-interface, the LBE/cover gas-interface and the absorber foils. In the following, we will describe these individual sample sets in more detail. Additional information on the individual samples is compiled in Table 1.

2.3.1 Samples from bulk LBE

Bulk LBE samples were obtained by core drilling in the top and bottom surfaces of the segments using a self-made core drill. The resulting samples were visually homogenous cylinders with a diameter of 2 mm and a length of 5 mm. From the 43 samples obtained in this way from the bulk, 16 samples covering the full height of the LBE-containing part of the target (i.e. from segments H02 to H07) were selected for analysis.

2.3.2 Samples from the LBE/steel-interface

LBE-steel interface samples were obtained using the same core drilling procedure, the only difference being the centre of the drill placed directly at the LBE-steel interface. In this way, samples were obtained that consisted of an LBE part and a steel part each corresponding to approximately a half cylinder with the dimensions mentioned above. For the analysis of ^{129}I and ^{36}Cl we selected six samples from the segments H03 to H06. For two of these samples (H05-D6(2)-b and H06-D2S) both the LBE and the steel part was available for analysis, while for the remaining samples only either the LBE part or the steel part was analysed. An important criterion for the selection of the samples was that they had a defined shape that allowed a reasonably precise estimation of the surface area of the LBE-steel interface region, since this quantity will be later used to estimate the total amount of the studied nuclides accumulated on the LBE-steel interface regions of the target.

2.3.3 Samples from the LBE/cover gas-interface

The third type of samples represents those sections of the target where the LBE was in contact with the Argon cover gas during operation. This set of samples is more heterogeneous than the bulk LBE and steel interface samples, both in the sense that it comprises materials of different nature taken from different locations in the upper part of the target and also in the sense that these samples do not consist of a single homogeneous phase or an interface with defined geometry, but they are composed of both LBE and another solid material, and most of them have an irregular shape. This set of samples comprises both material from the surface of solidified LBE found in the section H07 of the target as well as material found sticking to the walls of certain parts of the sections H07 and H08. Unfortunately, it was not possible to completely separate the LBE and the solid contamination by mechanical or chemical means. This heterogeneity makes it desirable to discuss more in detail the mechanisms that probably lead to the formation of these types of samples: During operation of the target, the free surface of the LBE was located in the lower part of the expansion volume represented by the section H08 (Figure 1). After the end of irradiation, the level of this free surface declined due to thermal contraction of the LBE, leaving the segment H08 virtually free of LBE, apart from some material that remained sticking to the steel walls. The latter is the origin of all the H08 samples analysed here. However, this material is not homogeneous. By visual inspection it became obvious that two different kinds of material were located in this region of the target. One type consists of solidified LBE that is contaminated with a dark solid. This sub-type of samples is represented in our analyses by two fragments of sample H08-U2 that have been separately analysed to obtain information on the uniformity of the nuclide distribution in this type of sample. The other type of sample from segment H08 (H08-U1-b) consists of grey and yellow coloured brittle solid material that had the appearance of a powder that is sintered to form a crust sticking to the steel wall. It seems likely that it consists to a substantial part of lead and/or bismuth oxides that are possibly held together by a certain amount of solidified LBE.

Finally, we studied two different samples from segment H07. Sample H07-U2 represents material that is similar to sample H08-U2. It was found sticking to the wall of a ring-shaped structure. Sample H07-S represents the solidified free surface of LBE that was found within another ring-shaped structure of H07. The complete surface of the LBE was covered with a thin layer of a dark solid material. Several samples were obtained from this surface using the core drilling technique. The samples obtained in this way consisted only to a small part of the dark deposit located on the top surface of the cylinder, while the major part represents the LBE located underneath. To obtain more information on the distribution of the studied nuclides between the dark deposit and the LBE, for the one sample of this type we separately analysed the top 0.5 mm of the sample cut using a scalpel, containing the dark layer, and also a part of the sample lying below the top surface. However, because of the rather crude cutting, even the "surface" part of the samples consisted of LBE to a large part, and no sample that was fully representative for the black deposit was obtained.

2.3.4 Samples from the absorber-foils in the expansion volume

In order to obtain information on possible iodine and chlorine release from the liquid metal, we additionally analysed samples from the absorber foils that were installed on the central rod in the target's expansion volume (H09, Figure 1). This absorber consisted of six layers of silver foil and one palladium foil, stacked onto each other, as shown in Figure 2. To obtain information on the uniformity of depositions from the gas phase, two samples, a and b, were taken on opposite sides of each foil as illustrated in Figure 2. For analysis, we used small pieces (5–46 mg) of each foil which were visually checked for not being contaminated by splashed LBE.

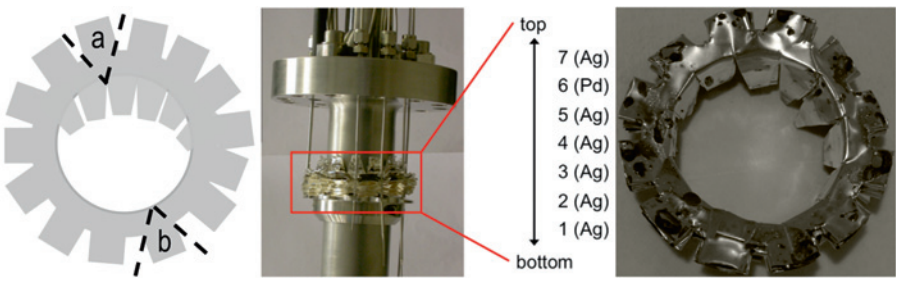

Fig. 2: Illustration of cutting sample series a and b from the absorber assembly. left: schematic view of sampling positions; middle: absorber foils mounted on the central rod before operation; right: photograph of absorber foils as retrieved after operation, showing visible contamination by splashed LBE.

2.4 Chemical separation of ^{36}Cl and ^{129}I from LBE and absorber foils

The method used for the separation of iodine and chlorine has been adapted from a previous one developed for the separation of halogens from irradiated Bi- and Pb-targets [16, 17]. 12 mg of LBE, together with iodine carrier (about 12 mg iodine, Woodward Iodine Corporation, USA) and chlorine carrier (10 mg chlorine in form of NaCl, from Merck) were dissolved in 5–7 ml 7 M HNO_3 in a three-neck-flask in an N_2 atmosphere at room temperature. After complete dissolution, the reaction mixture was heated up to 100 °C. Iodine and chlorine were distilled into an aqueous hydrazine solution. The hydrazine solution was acidified with 7 M HNO_3 and $AgNO_3$ was added, forming unsoluble AgI and AgCl. The precipitate was filtered and re-dissolved in NH_3 (25%). Only AgCl is soluble in NH_3. AgI was filtered off and the residue was washed 3 times with 5 ml 7 M HNO_3 and dried for at least 24 h at 80 °C. The AgCl fraction was acidified with 7 M HNO_3 to re-precipitate AgCl. The precipitate was washed with bi-distilled H_2O and dried for about 24 h at 80 °C.

Samples consisting of steel with no or only tiny amounts of adherent LBE where treated as well with 7 M HNO_3 to dissolve LBE and also deposited I and Cl adhering to the steel surface, as described above for bulk LBE. The steel remains undissolved under this treatment.

Additionally, small pieces (between 5–46 mg) from the absorber foils (Pd and Ag) were analysed. The Pd foil was first dissolved in 7 M HNO_3 and afterwards the distillation of chlorine and iodine in a N_2 atmosphere was performed, as described above, using between 10 and 30 mg iodine and 10 mg chlorine carrier. The Ag foils were dissolved in 7 M HNO_3 and afterwards iodine carrier (10–30 mg) and chlorine carrier (10 mg) in hydrazine solution were added leading to a precipitation of AgI and AgCl. Since evaporation of the halogens is not expected under these conditions, the distillation step was omitted. The reprocessing for ^{129}I and ^{36}Cl from the absorber was the same as described above for LBE samples.

Corresponding blank samples for ^{129}I and ^{36}Cl were prepared employing identical procedures as described above, using about 12 mg of inactive LBE from the batch of LBE used for the MEGAPIE target. For the analysis of the surface samples six blank experiments were performed after the experiment series. In order to conservatively estimate the background, the highest ratios of ^{129}I/I and ^{36}Cl/Cl, respectively, were used. For the analysis of bulk samples and the Pd-foil of the absorber, blanks were performed before each separation.

2.5 AMS measurement

Both isotopes were measured at the Laboratory of Ion Beam Physics at ETH Zurich. For details of the measurement techniques and the facilities see [18].

^{129}I/I ratios were determined using the 0.6 MV TANDY AMS facility. The AgI sample is loaded in a metallic cathode and bombarded with caesium ions, which sputter and ionize the iodine atoms, extracting negative iodine ions. Helium is used as gas stripper, generating 2+ charge state for iodine after stripping. Background effects were evaluated using iodine blanks (Iodine, from Woodward Iodine Corporation, USA). ^{36}Cl was measured at the 6 MV EN TANDEM accelerator with a Cs gun ion source. The Cs vapour is ionized on a hot frit and the sample is sputtered with the Cs beam. The sample material (AgCl) is pressed on a flat Cu sample holder that is equipped with a Ta inlay. At the low energy side, negative Cl ions are measured in offset Faraday cups after the low energy magnet. The main challenge in ^{36}Cl AMS measurements is its discrimination from the isobar ^{36}S. This is done in a multi-anode gas ionization detector and thus requires high ion energies. The TANDEM is running at 5.8 MV and ions are analysed in charge state 7+ after foil stripping, resulting in an ion energy of 46.4 MeV [18].

2.6 Uncertainties

The uncertainty of each single measurement was calculated using standard error propagation methods. We consider the uncertainties from the Eppendorf pipette (±0.8%), from the carrier (chlorine: ±4.22%, resulting from weighing the sample and from pipetting the NaCl solution; iodine: ±0.7%–1.2%, from weighing), from the uncertainty in the yield of AgI and AgCl precipitation (±0.3%–2.5%), and from the AMS measurement (±2%–19%).

3 Results

3.1 ^{36}Cl and ^{129}I concentration in bulk samples

The results obtained for ^{129}I activity concentrations found in the bulk samples are visualized in Figure 3, ordered according to the flow direction of the LBE, starting with samples where the LBE was flowing from the nuclear reaction zone upwards through the pump and coming down through the heat exchanger back to the lower part of the

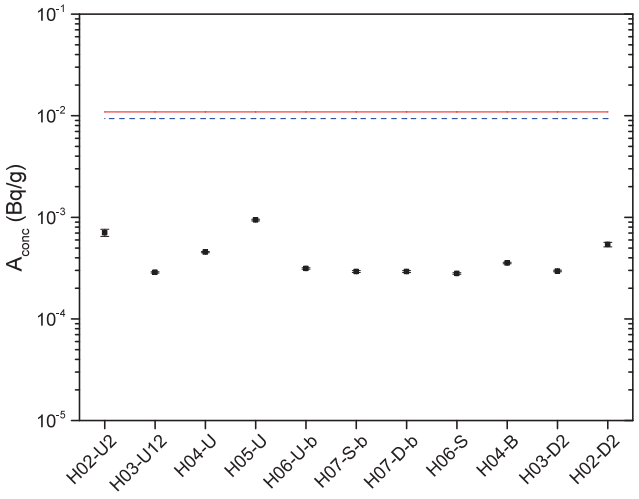

Fig. 3: Activity concentration of ^{129}I in individual samples of bulk LBE from MEGAPIE target compared to activity concentrations obtained from FLUKA (red line) and MCNPX (dashed blue line) predictions assuming homogeneous distribution of all produced ^{129}I in the LBE [10]. The samples are arranged according to the LBE flow, starting with upstream samples (H02 to H07) followed by downstream samples (H07 to H02).

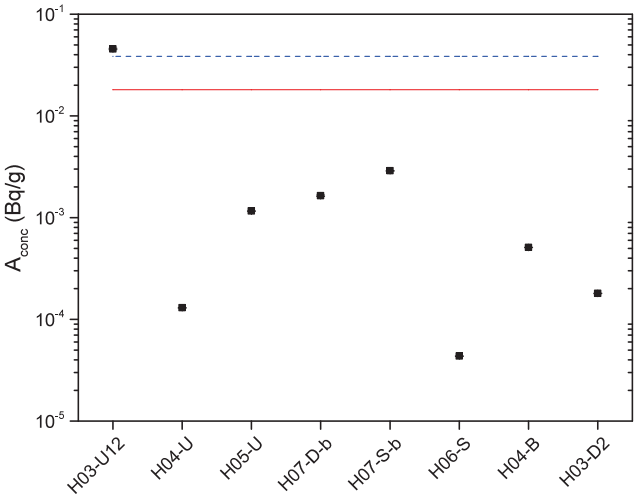

Fig. 4: Activity concentration of ^{36}Cl in bulk samples from MEGAPIE target compared to FLUKA (red line) and MCNPX (dashed blue line) predictions [10].

target. The distribution of ^{129}I in these samples was found to be rather homogeneous. We also do not observe any systematic change of the activity concentration along the flow direction of the liquid metal. From the rather homogeneous distribution of ^{129}I within the bulk LBE we conclude that we can derive a meaningful value for the total ^{129}I content of the LBE by averaging the activity concentrations of all analysed samples and multiplying with the total mass of LBE present in the target, 845 kg. The total content of ^{129}I in the bulk LBE derived in this way amounts to 295 ± 18 Bq. This corresponds to approx. 3% of the amount of ^{129}I that was predicted by nuclear physics codes (FLUKA: 9220 Bq; MCNPX: 7900 Bq) [10], indicated in Figure 3. While the theoretical predictions obtained by the two nuclear codes agree well with each other, the measured activity concentrations are 1.5 to 2 orders of magnitude lower.

The activity concentrations of ^{36}Cl found in the analysed bulk LBE samples are shown in Figure 4. The measured values show a much larger scatter compared to the activity concentrations found for ^{129}I. In particular, one sample (H03-U12) shows an extremely high content. The large scatter raises questions concerning the representativeness of the sample set and thus makes a derivation of the total content of ^{36}Cl by averaging and summing up over the total target mass questionable. Averaging over all eight samples gives a mean value of $(6.6 \pm 5.6) \times 10^{-3}$ Bq/g. Summing up over the target mass this results in 5.6 ± 4.8 kBq, representing 23% of the mean of the predicted amounts of this nuclide [10] (FLUKA: 32.5 kBq; MCNPX: 15.3 kBq, mean value 23.9 kBq). Assuming sample H03-U12 is an exceptional specimen that is not representative for the bulk LBE and thus averaging the remaining seven samples, we obtain a mean activity concentration of $(9.9 \pm 4.1) \times 10^{-4}$ Bq ^{36}Cl per gram LBE. Summing up for the total LBE in the target, this corresponds to $(8.4 \pm 3.4) \times 10^{2}$ Bq, representing 3.5% of the mean value of the predicted amount. In this case, we arrive at a similar discrepancy between prediction and chemical analysis for ^{36}Cl and ^{129}I.

There are numerous mechanisms and phenomena that can explain how and why an enrichment of a certain element could occur at various locations in the target. These will be discussed later in this paper in context with all the available results obtained for different sample types. However, although in principle the effect can be explained, the question of how representative the samples are concerning the ^{36}Cl-content cannot be answered in a fully satisfactory way. Therefore, the results presented above for ^{36}Cl in the bulk have to be taken with caution.

3.2 ^{129}I and ^{36}Cl in LBE/steel-interface samples

The radionuclides in these samples are most probably accumulated in thin surface layers on both LBE and steel parts of the samples that represent the contact surface. This is intuitively clear for the steel specimens: It is unlikely that the radionuclides produced in the LBE could

diffuse into the steel under the prevailing conditions. Indeed, γ-spectrometric analysis of other radionuclides, e.g. ^{173}Lu [15, 19], in the same steel samples used here showed that these nuclides are present as a layer on the steel surface that can be almost completely removed (>98%) by the leaching procedure described in the experimental section. We assume that the ^{129}I and ^{36}Cl detected on the steel specimens are also associated with this thin layer located on the interface of LBE and steel, and that they were removed completely from the steel surface by the leaching procedure. For the LBE part of the interface samples, we generally found much higher activities per mass unit compared to the bulk LBE samples (factor 30 to 100 for ^{129}I, factor of approx. 4 to 50 for ^{36}Cl), see Table 2. This is consistent with the assumption that a thin deposition layer containing the radionuclides formed during operation of the target at the LBE steel interface. When samples are taken from the interface by core drilling and afterwards breaking apart the steel and LBE part, variable fractions of this deposition layer stick to both the LBE and the steel part.

As a consequence of this multi-phase nature of the interface samples, it does not make sense to present the results of analysis in form of activity concentrations. Instead, we give the results in Table 2a in form of total activity per sample as well as activity per unit surface. The interface surface of the samples was determined by measuring the dimensions of the samples. As an example, the interface area of LBE with the steel container material in a complete and fully symmetrical core drill of 2 mm diameter and 5 mm length, as depicted in Figure 5 will be 1.0×10^{-5} m^2.

However, all of the analysed samples were not fully ideal. Most of them were drilled slightly asymmetrically. Furthermore, in many cases the core was slightly shorter than the nominal 5 mm. Thus, all of the samples investigated had a smaller area than the ideal 1.01×10^{-5} m^2. In a few cases, only fragments of a core were analysed. We assume that the uncertainty of the estimation of the surface area is smaller than 15%.

The ^{129}I content on the surface of the samples varies within one order of magnitude, from a few tens of Bq/m^2 to a few hundred Bq/m^2. We observe the highest values of ^{129}I surface activity in samples from the lower part of the heat exchanger, i.e. at places where the down flowing LBE was in contact with a cold surface and therefore cooled down to the lowest temperature within the loop. However, with the few samples studied here and the substantial deposition of ^{129}I also observed in the other parts of the target, a preferred deposition of iodine in the temperature gradient of the heat exchanger cannot be identified.

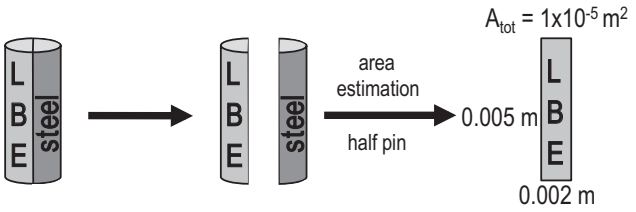

Fig. 5: Illustration of a LBE/steel-interface sample, broken into two parts. The area of one part is given [19].

The values determined for the surface activities of ^{36}Cl in the same samples scatter much stronger than those for ^{129}I. Measurable activities were only detected in the samples H03-U6 (LBE part), H05-U4-b (steel part), H06-D2S(1) (both LBE and steel part) and H06-D2S(2) (steel part). On all other samples, the isotopic ratio ^{36}Cl/^{stable}Cl was in the region or below the blank. For the two samples representing the LBE-part of the interface where the ^{36}Cl activity was significantly above the blank value, the measured values indicate strong enrichment of this nuclide compared to the bulk LBE. However, for the remaining LBE samples from the interface we did not detect significant amounts of ^{36}Cl. Interestingly, among them are the samples where the highest surface concentrations of ^{129}I were found. The amount of ^{36}Cl that was sticking to the steel parts of the interface samples was found to be lower compared to that detected on the LBE parts. The highest surface concentration was found in sample H05-U4-b, with the other three steel samples showing an order of magnitude lower surface concentration, or in one case even no significant amount of ^{36}Cl at all.

To obtain a crude estimate of the total amount of ^{129}I and ^{36}Cl associated with the surface layer, the averages of the surface activities found for both the steel and the LBE samples were extrapolated to the total target surface of 16 m^2 [20], and then the total activity sticking to the target walls was calculated by summing up both contributions. This estimation relies on the assumption that the average of the surface activities of the studied samples is representative for the complete target. With the few samples studied and the large scatter observed in the analysis results, this assumption is rather rough, in particular for ^{36}Cl. However, the assessment should allow at least concluding on the order of magnitude of the total ^{129}I and ^{36}Cl content in these interface samples. The large scatter of the analysis results and the small sample number are reflected in the large uncertainties given, which were derived from the standard errors of the mean values of individual sample sets. In Table 2b the total activity obtained by this extrapolation is compared to the predictions of the nuclear codes. The total ^{129}I activity obtained is 3.7 ± 2.0 kBq,

Table 2a: Results of ^{129}I and ^{36}Cl analysis in steel and LBE parts of interface samples. Activities calculated to EOB. Averages of the surface activity concentrations are given for the LBE and steel part.

Sample	Material	Sample mass [g]	Interface area [m^2]	Activity ^{129}I [Bq][(a)]	^{129}I activity per unit surface [Bq/m^2]	activity ^{36}Cl [Bq][(a)]	^{36}Cl activity per unit surface [Bq/m^2]
H03-U6	LBE	0.0399	8×10^{-6}	$(4.4 \pm 0.1) \times 10^{-4}$	$(5.5 \pm 0.2) \times 10^{1}$[(a)]	$(1.5 \pm 0.06) \times 10^{-2}$	$(1.8 \pm 0.08) \times 10^{3}$[(a)]
H06-D2S(1)		0.0107	8×10^{-6}	$(4.0 \pm 0.08) \times 10^{-4}$	$(5.0 \pm 0.1) \times 10^{1}$[(a)]	$(6.0 \pm 0.3) \times 10^{-3}$	$(7.5 \pm 0.4) \times 10^{2}$[(a)]
H06-D2S(2)		0.0069	8×10^{-6}	$(2.9 \pm 0.2) \times 10^{-4}$	$(3.6 \pm 0.2) \times 10^{1}$[(a)]	$(2.5 \pm 0.3) \times 10^{-4}$[(c)]	$(8.2 \pm 0.9) \times 10^{1}$[(a)]
H05-D22		0.0444	5×10^{-6}	$(1.3 \pm 0.02) \times 10^{-3}$	$(2.7 \pm 0.05) \times 10^{2}$[(a)]	$(2.5 \pm 0.3) \times 10^{-4}$[(c)]	$(2.7 \pm 0.3) \times 10^{2}$[(a)]
H05-D6-b		0.0450	5×10^{-6}	$(6.2 \pm 0.2) \times 10^{-4}$	$(1.2 \pm 0.04) \times 10^{2}$[(a)]	$(2.5 \pm 0.3) \times 10^{-4}$[(c)]	$(1.3 \pm 0.2) \times 10^{2}$[(a)]
Average					$(1.1 \pm 0.4) \times 10^{2}$[(b)]		$(3.0 \pm 0.2) \times 10^{3}$[(b)]
H05-U4-b	Steel	0.0347	8×10^{-6}	$(2.2 \pm 0.06) \times 10^{-4}$	$(2.8 \pm 0.07) \times 10^{1}$[(a)]	$(2.3 \pm 0.09) \times 10^{-3}$	$(2.9 \pm 0.1) \times 10^{2}$[(a)]
H06-D2S(1)		0.0075	8×10^{-6}	$(8.3 \pm 0.1) \times 10^{-4}$	$(1.0 \pm 0.02) \times 10^{2}$[(a)]	$(7.6 \pm 0.4) \times 10^{-5}$	9.5 ± 0.4[(a)]
H06-D2S(2)		0.0169	8×10^{-6}	$(1.3 \pm 0.2) \times 10^{-4}$	$(1.6 \pm 0.3) \times 10^{1}$[(a)]	$(6.7 \pm 0.3) \times 10^{-5}$	8.3 ± 0.4[(a)]
H05-D6-b		0.0194	5×10^{-6}	$(1.8 \pm 0.07) \times 10^{-3}$	$(3.6 \pm 0.1) \times 10^{2}$[(a)]	$(2.5 \pm 0.3) \times 10^{-4}$[(c)]	$(1.1 \pm 0.1) \times 10^{2}$[(a)]
Average					$(1.3 \pm 0.8) \times 10^{2}$[(b)]		$(2.2 \pm 1.) \times 10^{2}$[(b)]

[(a)] Uncertainties for the values given for the individual samples are standard errors.
[(b)] Uncertainties given for the averages are standard errors of the mean value.
[(c)] Detection limit.

Table 2b: Results of ^{129}I and ^{36}Cl analysis in steel and LBE parts of interface samples. Activities corrected to EOB. Averages of the surface activity concentrations for the LBE and steel part, given in Table 2a (Bq/m^2) were extrapolated to the target's total inner surface, 16 m^2, and summed up.

Sample	Material	^{129}I mean activity extrapolated to total inner surface [Bq][(a)]	^{36}Cl mean activity extrapolated to total inner surface [Bq][(a)]
H03-U6 H06-D2S(1) H06-D2S(2) H05-D22 H05-D6-b	LBE	$(1.7 \pm 0.7) \times 10^{3}$	$(9.8 \pm 5.2) \times 10^{3}$
H05-U4-b H06-D2S(1) H06-D2S(2) H05-D6-b	Steel	$(2.0 \pm 1.3) \times 10^{3}$	$(1.7 \pm 1.1) \times 10^{3}$
Sum over total inner LBE and steel surface		$(3.7 \pm 2.0) \times 10^{3}$	$(1.2 \pm 0.6) \times 10^{4}$
% of prediction[(b)]		43 ± 23	48 ± 26

[(a)] Uncertainties given for the averages are standard errors of the mean values.
[(b)] Average of FLUKA and MCNPX calculation.

corresponding to 44 ± 23% of the averaged predictions of the two nuclear physics codes [10]. For ^{36}Cl we obtain 12 ± 6 kBq, corresponding to 48 ± 26% of the predicted amount.

3.3 ^{129}I and ^{36}Cl in the LBE/cover gas-interface samples

All samples taken from those parts representing the LBE/cover gas-interface were not single phase but rather a conglomerate of LBE and another solid material (in the following referred to as "deposit") in varying proportions. This deposit was known from γ-spectrometric analyses [15] to be enriched in electropositive nuclear reaction products. It was suspected that a similar enrichment could also have occurred for iodine and chlorine. Unfortunately, it was not possible to fully separate the deposit from the LBE by mechanical or chemical means. Thus, no explicit data on the radionuclide content of the pure LBE-free deposit could be obtained.

The results are compiled in Table 3. Because of the multiphase nature of the samples we cannot provide activity concentrations as in case of the bulk samples. Therefore, the absolute activities A_{exp} found in fragments of a mass of $m_{analysed}$ are given for each sample together with the total mass of the retrieved sample, m_{sample}. If we look at the ratios $A_{exp}/m_{analysed}$ found for the halogen nuclides and compare them to the activity concentrations obtained in the bulk LBE (Section 3.1), we find that sample H07-S(b) contains an amount of ^{129}I similar to the activity concentration found in the bulk samples. The values of activity per mass unit of the other four samples vary strongly, being 1 to 3 orders of magnitude higher than the bulk activity concentrations. These results confirm that the major fraction of the ^{129}I and ^{36}Cl found in the interface samples is associated with the black, grey or yellow solids con-

Table 3: ^{129}I and ^{36}Cl results from LBE/cover gas-interface samples. Activities corrected to EOB.

	m_{sample} [mg]	$m_{analysed}$ [mg]	fraction F of individual sample/total	^{129}I A_{exp} [Bq]	^{36}Cl A_{exp} [Bq]	^{129}I A_{typ} [7] [Bq]	^{36}Cl A_{typ} [7] [Bq]
H07-U2[1]	226.1	14.7	0.01[5]	$(1.7 \pm 0.05) \times 10^{-4}$	$(6.8 \pm 0.5) \times 10^{-4}$	$(2.6 \pm 0.08) \times 10^{-1}$	$(1.1 \pm 0.1) \times 10^{1}$
H07-S(a)[2]	10.3	10.3	1.1×10^{-4} [6]	$(9.2 \pm 0.9) \times 10^{-5}$	$(2.0 \pm 0.2) \times 10^{-4}$	$(8.8 \pm 0.8) \times 10^{-1}$	$(1.9 \pm 0.2) \times 10^{1}$
H07-S(b)[2]	14.6	14.6	1.1×10^{-4} [6]	$(4.2 \pm 0.4) \times 10^{-6}$	$(2.5 \pm 0.3) \times 10^{-5}$ [9]	$(4.0 \pm 0.3) \times 10^{-2}$	$(2.4 \pm 0.3) \times 10^{1}$
H08-U1-b[3]	159.3	12.0	0.05[5]	$(1.4 \pm 0.1) \times 10^{-4}$	$(1.5 \pm 0.1) \times 10^{-2}$	$(3.8 \pm 0.2) \times 10^{-2}$	$(3.9 \pm 0.02) \times 10^{1}$
H08-U2[1]	172.2	14.2	0.7[5]	$(1.0 \pm 0.06) \times 10^{-3}$ [4]	$(8.9 \pm 0.4) \times 10^{-3}$	$(1.6 \pm 0.1) \times 10^{-2}$ [4]	1.1 ± 0.01
					Total activity in free surface A_{tot} (Bq)[8]	1.2 ± 0.1	$(10.4 \pm 0.6) \times 10^{1}$

[1] LBE contaminated by dark deposit, remainder of free surface, sticking to the steel wall; [2] core drill in free surface: (a) top of core drill containing the dark deposit; (b) LBE from approx. 500 μm below free surface. [3] brittle grey and yellow coloured material, most likely oxide crust deposited on the steel wall from the free surface during level changes. [4] mean of 2 independend measurements. [5] Based on visual inspection, samples H07-U2, H08-U1-b and H08-U2 represent fractions F of approx. 0.01, 0.05 and 0.7 of the total material of their kind present in the target, respectively. [6] Ratio of top surface of sample H07-S, containing the dark deposit, to the total LBE free surface derived from construction drawings. [7] Total activity contained in the material represented by the sample: $A_{typ} = A_{exp} \times m_{sample}/m_{analysed} \times \frac{1}{F}$. [8] $A_{tot} = A_{typ,\,H07\text{-}U2} + A_{typ,\,H07\text{-}S(a)} + A_{typ,\,H08\text{-}U1\text{-}b} + A_{typ,\,H08\text{-}U2}$. [9] detection limit.

stituting a variable fraction of these samples (see section 2.3.3). Sample H07-S(b) had the surface deposit removed and thus corresponds to bulk LBE. The largest activities per unit mass of both nuclides are found in the material that was sticking to the walls of segment H08 (see Table 3; H08-U1-b for ^{36}Cl, H08-U2 for ^{129}I).

In the following, we roughly estimate the total amount of ^{129}I and ^{36}Cl associated with the depositions in the top part of the target, corresponding to the free surface of LBE and its remainders sticking to the walls of construction materials. For this purpose, we first estimate the activity of each nuclide associated to the four different free surface-related types of material, using knowledge from construction drawings, visual inspection of the respective target sections during sampling and in some cases conservative assumptions.

For the sample taken by core drilling in the solidified LBE free surface itself (H07-S) we know the area of the top surface of the cylinder. By relating this area (3.14×10^{-6} m^2) to the surface area of the ring structure that contained the LBE free surface (0.03 m^2) we can extrapolate to the activity contained in that ring structure by dividing the measured activity by the ratio of cylinder top surface to the total LBE free surface, 1.1×10^{-4}.

For material similar to the sample H07-U2, we estimate from visual inspection during the sampling that we have retrieved about 10% of this LBE contaminated with a dark solid from the ring structure it was located in. Sample H07-U2 itself constituted about 10% of the retrieved material, and thus to a fraction of 0.01 of the total material of this type present in the target. To estimate the amount of the studied nuclides in this material, we assumed that the analysed part (14.7 mg) is representative for the complete sample (226.1 mg), and moreover also for the entire material of this kind present in the target. Then, the activity associated to this type of material can be estimated by dividing the activity found in the analysed part of the sample by the mass ratio and the fraction estimated above.

Sample H08-U1-b consisted of grey and yellow deposit sticking to the central rod located within the expansion volume of the target. From visual inspection we can state that we were able to retrieve the major part of this material, i.e. at least 50% (1.6 g). For our conservative evaluation we use this fraction. The sample studied here represents 10% of this material. The activity in this material was estimated in a similar way as outlined above for sample H07-U2, assuming that the analysed part of the sample (12.0 mg) is representative for the complete sample (159.3 mg) as well as for all the material of this type.

Only a small amount of material similar to sample H08-U2 was found in the target. This material was completely retrieved, amounting to 0.24 g, sample H08-U2 representing roughly 70% of it. The content of ^{129}I and ^{36}Cl in the material of this type was estimated assuming that the analysed part of the sample (14.2 mg) is representative for all material of this type, as described above for samples H07-U2 and H08-U1-b.

The results of scaling up the analytical data to the content of ^{129}I and ^{36}Cl in the individual types of materials are compiled in columns 7 and 8 of Table 3. Finally, the total activity of each nuclide associated to the LBE free surface and its remainders sticking to the walls is calculated as the sum over the different types. This sum amounts to 1.2 ± 0.1 and 104 ± 6 Bq for ^{129}I and ^{36}Cl, respectively,

corresponding to 0.01 to 0.4% of the activities predicted by nuclear physics codes. Since only one measurement per sample type exists, the assumption that the analysed part of the samples is really representative for the entire amount of material of the respective type could be questioned. However, the values estimated are so low that we still can certainly state that, though there is clearly an enrichment compared to the bulk, the contribution of ^{129}I and ^{36}Cl located in samples originating from the LBE free surface to the total amount of these nuclides in the target can be neglected.

3.4 ^{129}I and ^{36}Cl activity adsorbed on the absorber foils in the gas plenum

Finally, we present results concerning the amount of ^{129}I and ^{36}Cl found on specimens from the silver and palladium foils installed in the expansion tank to trap volatile radionuclides that are potentially released to the cover gas. Generally, the results obtained from the two specimen analysed from each foil agreed well, indicating that the distribution of the two nuclides over the individual foils is rather homogeneous. Thus, we consider the average of the two experimental values representative for the individual foils and integrate the averaged activity concentrations over the mass to obtain an estimate for the total content of the individual foils. The resulting activity values obtained for ^{129}I and ^{36}Cl in each of the seven different foils (six Ag foils and one Pd foil) are compiled in Table 4.

We cannot detect any systematic trend in the distribution of ^{129}I and ^{36}Cl across the different foils. The total acitivities adsorbed on the absorber obtained by summing up over all foils amount to 0.38 ± 0.01 Bq for ^{129}I and 12 ± 0.51 Bq for ^{36}Cl, respectively. These values are much smaller than the amount found in the LBE/steel interface samples and correspond to fractions of 0.004% and 0.05% of the predicted total production for ^{129}I and ^{36}Cl, respectively.

Table 4: Total activities for ^{129}I and ^{36}Cl in the different absorber foils, obtained from mean value of two measurements for each absorber foil by integrating over the mass.

Absorber foil	m [g]	^{129}I A [Bq]	^{36}Cl A [Bq]
1 (Ag)	9.6299	$(36.5 \pm .9) \times 10^{-3}$	$(14.9 \pm 0.6) \times 10^{-1}$
2 (Ag)	9.6875	$(10.4 \pm .4) \times 10^{-2}$	$(16.3 \pm 0.7) \times 10^{-1}$
3 (Ag)	9.3945	$(3.4 \pm 0.2) \times 10^{-2}$	$(8.1 \pm 0.4) \times 10^{-1}$
4 (Ag)	9.3988	$(4.1 \pm .1) \times 10^{-2}$	$(17.5 \pm 0.7) \times 10^{-1}$
5 (Ag)	9.8407	$(3.4 \pm .3) \times 10^{-2}$	$(11.0 \pm 0.5) \times 10^{-1}$
6 (Pd)	2.3433	$(6.1 \pm 0.2) \times 10^{-2}$	$(7.1 \pm 0.4) \times 10^{-1}$
7 (Ag)	9.6419	$(6.4 \pm 0.1) \times 10^{-2}$	$(44.1 \pm 1.8) \times 10^{-1}$
Sum		0.38 ± 0.02	12 ± 0.5

4 Discussion

Samples from the MEGAPIE target representing the bulk LBE, the interface of LBE with the steel walls of the target container and with the cover gas as well as samples from absorber foils located in the cover gas space were analysed for ^{129}I and ^{36}Cl. The individual contributions of the four different sample types to the total radioactivity were roughly estimated. The results of this estimation are summarized in Table 5a and b and compared to predictions on the radionuclide production during the MEGAPIE irradiation obtained by two different nuclear physics codes employing different nuclear models [10]. We observe a reasonably good agreement of analytical data with the predictions.

For ^{129}I, the major part is clearly found to be deposited on the steel walls of the liquid metal container. Bulk samples contain only a minor fraction of the total ^{129}I detected in the target. A similar trend is also observed for ^{36}Cl, with the situation being less clear in this case because of the large scatter of the data in both bulk and LBE/steel-interface samples. On the free surface of the LBE that was in contact with the cover gas during operation of the target, a strong enrichment of the two halogen nuclides compared to the bulk is observed. However, the contribution of this fraction to the total radioactivity is small because the area of this LBE cover gas interface is much smaller than the target inner surface and therefore negligible. A similarly small fraction of ^{129}I and ^{36}Cl was found on the noble metal absorber foils that were installed in the expansion tank to trap volatile elements released from the LBE.

The small amounts of the halogen nuclides found on the absorber foils do not indicate a substantial release of the halogens to the cover gas. However, in principle released halogens may have passed the absorber foils and deposited on the walls of the expansion tank and the cover gas system or even have been released from the target system with the exhaust gas that was extracted typically once a month during operation. On the other hand, in gas samples taken during the operation of the target only traces of iodine isotopes were detected, too low to extract quantitative information [10]. Furthermore, also in the exhaust gas monitoring no large quantities of iodine isotopes were found [10]. Finally, in dedicated experiments on the evaporation of iodine from LBE [21] it was shown that significant evaporation occurs only at temperatures >500 °C, much

Table 5a: Summary of ^{129}I activity distribution over the different types of samples.

	Estimated total activity [Bq]	Predicted activity[a] [Bq]	% of predicted amount	% of estimated total activity
Bulk	295 ± 18	8560	3.4 ± 0.2	7
LBE/cover gas interface	1.2 ± 0.1		$(14 \pm 1) \times 10^{-3}$	0.03
LBE/steel interface	$(37 \pm 20) \times 10^{2}$		43 ± 23	93
Absorber	$(38 \pm 2) \times 10^{-2}$		$(44 \pm 2) \times 10^{-4}$	0.01
Sum	3997 ± 2018		47 ± 24	

[a] Average of two calculations using different nuclear models.

Table 5b: Summary of ^{36}Cl activity distribution over the different types of samples

	Estimated total activity [Bq]	Predicted activity[a] [Bq]	% of predicted amount	% of estimated total activity
Bulk	$(56 \pm 48) \times 10^{2}$	239×10^{2}	23 ± 20	32
	$(84 \pm 34) \times 10^{1}$ [b]		3.5 ± 1.4[b]	4.8[b]
LBE/cover gas interface	104 ± 6		$(4.4 \pm 0.3) \times 10^{-1}$	0.6
				0.8[b]
LBE/steel interface	$(1.2 \pm 0.6) \times 10^{4}$		48 ± 26	68
				92[b]
Absorber	12 ± 0.5		$(50 \pm 2) \times 10^{-3}$	0.07
				0.09
Sum	$(177 \pm 108) \times 10^{2}$		71 ± 46	
	$(130 \pm 63) \times 10^{2}$ [b]		52 ± 27[b]	

[a] Average of two calculations using different nuclear models [10].
[b] Assuming sample H03-U12 contains an exceptionally high amount of ^{36}Cl which is not representative for bulk LBE (see text).

higher than the temperatures of the LBE free surface in the MEGAPIE target during operation (approx. 280 °C [10]). Putting all this information together, it seems unlikely that a large fraction of the halogens was released to the cover gas.

Nevertheless, it is noteworthy that the amount of ^{129}I and ^{36}Cl accumulated on the absorber foils is similar to that estimated for the total LBE/cover gas-interface, i.e. an area where the halogens were clearly found to be enriched compared to the bulk. Furthermore, the fraction of the total ^{129}I amount on the absorber (0.01%) is much higher than the fraction estimated to be present in the expansion tank under equilibrium conditions (5×10^{-14}%) [22]. Both facts clearly indicate a certain affinity of the noble metal absorber foils to halogens.

The distribution of ^{129}I and ^{36}Cl in the bulk, LBE/steel-interface and LBE/cover gas-interface samples is similar to that observed for lanthanide nuclides [19]. Lanthanides are incorporated into solid layers, most likely of oxidic nature, that are formed or are already present at the interfaces. The results of the present work indicate that the same solids are also enriched in ^{129}I and ^{36}Cl. In contrast to the strongly electropositive lanthanides, the electronegative halogens will not be present in such layers in a cationic form. However, they are highly reactive towards metals [23] and form stable halogenides with almost all metals, among them the components of the liquid metal matrix, lead and bismuth [24]. Thus, it is an obvious conclusion that iodine and chlorine nuclides, after they have been formed by nuclear reactions within the LBE, will chemically react with the matrix material. Because of the complexity of the liquid metal target system [13, 14], e.g. oxygen, corrosion and spallation products. Therefore, the final reaction product will not be a simple single phase solid such as PbX_2 (X = Cl, I), but rather a complex phase or even multi-phase mixture where iodine and chlorine are probably present in anionic form. It seems plausible that in such a solid, iodine and chlorine could be bound in a similar way as in the oxyhalogenides of Pb and Bi [25], which are a well-known class of stable compounds, some of the mixed Pb/Bi phases even occurring as minerals, e.g. $PbBiClO_2$ [26] or $PbBiIO_2$ [27]. Such materials are of highly polar or even ionic nature and thus will tend to be insoluble in liquid metals. Based on this reasoning it is

possible to qualitatively explain the accumulation of ^{129}I and ^{36}Cl observed in the interface samples studied here.

The formation of insoluble phases enriched in impurities may also be the cause for inhomogeneity observed in the radionuclide content in the bulk samples: The precipitation of insoluble phases from the liquid metal can also result in the formation of particles that remain suspended in the liquid metal, or such particles are produced by erosion of the material deposited on the walls of the target container. Depending on particle size and distribution in the liquid metal, the individual samples from bulk LBE could contain more or less of such particles enriched in radioactive impurities, or particles of significantly different size, leading to the observed scatter in the analytical data.

Particles containing impurities may even have been present already before the operation of the target. If this was indeed the case, and these particles contained a chlorine impurity, it could explain the fact that the scatter of ^{36}Cl data is much larger compared to the ^{129}I data: The chlorine impurity would be subject to neutron capture under irradiation, resulting in exceptionally high concentrations of ^{36}Cl in such particles. On the other hand, even if this particle would contain an iodine impurity as well, it would not be enriched in ^{129}I because a similar nuclear reaction pathway for the production of ^{129}I from stable iodine does not exist.

Thus, qualitatively, the phenomena leading to inhomogeneity of the halogen radionuclide distribution in the MEGAPIE liquid LBE target can be explained by simple chemical plausibility considerations. However, details of the underlying mechanisms cannot be extracted from the present data but remain to be explored in dedicated studies of the associated phenomena.

5 Summary and conclusions

Both the total amount and the distribution of ^{129}I and ^{36}Cl in the MEGAPIE target were determined from samples representing the bulk LBE, the interface of LBE with the steel walls of the target container, interface of LBE with the cover gas and noble metal foils installed in the gas phase for catching volatile radioactive species. The experimental results agree reasonably well with the predictions of nuclear physics codes, as shown in the Table 5a and b.

The amounts of ^{129}I and ^{36}Cl found on the absorber foils installed in the cover gas are in the order of maximum 0.1% of the total amount of these nuclides present in the target. Together with results from gas phase analysis and other supporting studies, this is compatible with the view that the major part of the halogens is retained in the target. Nevertheless, a comparison with the extremely small gas phase concentrations estimated for iodine in the MEGAPIE expansion tank reveals an affinity of the noble metals for halogens. Thus, they represent promising filter materials for the development of gas purification systems for ADS and similar installations.

The two halogen nuclides were found to be depleted in the bulk and accumulated on the interfaces, predominantly on the steel walls of the target container. Especially for ^{36}Cl, a strongly inhomogeneous distribution was found even in the bulk LBE that seems only explainable by assuming the presence of particles enriched in chlorine precipitating in the LBE. A chemically plausible explanation for this depletion, accumulation and precipitation effects is suggested. However, a detailed assessment of the mechanisms involved in the depletion and accumulation phenomena is beyond the scope of the present study. Thus, it remains the subject of further dedicated studies to prove or refute the suggested chemical explanation. This could be achieved e.g. by characterising the deposited layers and suspended particles themselves and by studying incorporation of radionuclides into them. Since the deposition processes observed here for the halogens but also in earlier studies for lanthanide nuclides may have significant operational consequences for the operation of future nuclear systems based on liquid LBE, such studies are certainly desirable.

Acknowledgement: The work was funded by the EC projects ANDES (Contract No. 249671), SEARCH (Contract No. 295736) and GETMAT (Contract No. 212175) in the frame of EURATOM FP7. We acknowledge the EU financial support.

References

1. Rubbia, C.: Particle accelerator developments and their applicability to ignition devices for inertial fusion. Nucl. Instrum. Methods Phys. Res. Sect. A **278**, 253 (1989).
2. Rubbia, C.: Inertial fusion: A contribution of accelerator technology to the energy problem? Nucl. Phys. A **553**, 375 (1993).
3. Gorse-Pomonti, D., Russier, V.: Liquid metals for nuclear applications. J. Non. Cryst. Solids **353**, 3600 (2007).
4. Handbook on Lead-Bismuth Eutectic Alloy and Lead. Properties, Materials Compatiblility, Thermal-hydraulics and Technologies. vol. NEA No. 6195. OECD Nuclear Energy Agency (2007).
5. Bauer, G. S.: Physics and technology of spallation neutron sources. Nucl Instrum. Methods Phys. Res. Sect. A **463**, 505 (2001).
6. Bauer, G. S., Salvatores, M., Heusener, G.: MEGAPIE, a 1 MW pilot experiment for a liquid metal spallation target. J. Nucl. Mater. **296**, 17 (2001).

7. Wagner, W., Gröschel, F., Thomsen, K., Heyck, H.: MEGAPIE at SINQ – The first liquid metal target driven by a megawatt class proton beam. J. Nucl. Mater. **377**, 12 (2008).
8. Wohlmuther, M., Wagner, W.: PIE preparation of the MEGAPIE target. J. Nucl. Mater. **431**, 10 (2012).
9. Zanini, L., Konobeyev, A. Y., Fischer, U.: Analysis of nuclide production in the MEGAPIE target. Nucl. Instrum. Methods Phys. Res. Sect. A **605**, 224 (2009).
10. Zanini, L., David, J.-C., Konobeyev, A. Y., Panebianco, S, Thiolliere, N.: Neutronic and Nuclear Post-Test Analysis of MEGAPIE. PSI Rep. Nr. 08-04, Paul Scherrer Inst., Villigen, Switzlerland (2008).
11. Fazio, C., Gröschel, F., Wagner, W., Thomsen, K., Smith, B. L., Stieglitz, R.: The MEGAPIE-TEST project: Supporting research and lessons learned in first-of-a-kind spallation target technology. Nucl. Eng. Des. **238**, 1471 (2008).
12. Bubelis, E., Coddington, P., Mikityuk, K.: Verification of the TRACE code against the MEGAPIE transient data. Ann. Nucl. Energy **35**, 1284 (2008).
13. Neuhausen, J., Schumann, D., Dressler, R., Eichler, B., Heinitz, S., Hammer, B.: Radiochemical Aspects of Liquid Metal Spallation Targets, p. 44, Proceedings of DAE-BRNS Symposium on Nuclear and Radiochemistry NUCAR-2011, Visakhapatnam (2011), India.
14. Neuhausen, J., Horn, S., Eichler, B., Schumann, D., Stora, T., Eller, M.: Mercury purification in the Megawatt Liquid Metal Spallation Target of EURISOL-DS. Eight Int. Top Meet. Nucl. Appl. Util. Accel. ACCAPP'07 Pocatello, Idaho (2007).
15. Hammer, B., Neuhausen, J., Boutellier, V., Linder, H. P., Shcherbina, N., Wohlmuther, M.: Analysis of the ^{207}Bi, ^{194}Hg/Au and ^{173}Lu distribution in the irradiated MEGAPIE target. J. Nucl. Mater. **450**, 278 (2014).
16. Schumann, D., Neuhausen, J., Michel, R., Alfimov, V., Synal, H.-A., David, J.-C.: Excitation functions for the production of long-lived residue nuclides in the reaction ^{nat}Bi(p; xn, yp), Z. J. Phys. G. Nucl. Part Phys. **38**, 065103 (2011).
17. Schumann, D., David, J. C., Cross sections and excitation functions for the production of long-lived radionuclides in nuclear reactions of lead and bismuth with protons. Nucl. Data Sheets **119**, 288 (2014).
18. Christl, M., Vockenhuber, C., Kubik, P., Wacker, L., Lachner, J., Alfimov, V.: The ETH Zurich AMS facilities: Performance parameters and reference materials. Nucl. Instrum. Methods Phys. Res. Sect. B Beam Interact. Mater. At. **294**, 29 (2013).
19. Hammer, B., Neuhausen, J., Boutellier, V., Wohlmuther, M., Türler, A., Schumann, D.: Radiochemical determination of rare earth elements in proton irradiated lead-bismuth eutectic. Anal. Chem. **87**, 5656 (2015).
20. Groeschel, F., Neuhausen, J., Fuchs, A., Janett, A.: Intermediate Safety report, Treatment of the Reference Accident Case, Deliverable D14 of WP1 of the MEGAPIE-TEST program, 5th EURATOM Framework program, Paul Scherrer Institute (2006).
21. Neuhausen, J., Eichler, B.: Investigations on the thermal release of iodine from liquid eutectic lead-bismuth alloy. Radiochim. Acta **94**, 239 (2006).
22. Neuhausen, J.: Gas phase concentrations of volatile nuclear reaction products in the MEGAPIE expansion tank. PSI Rep TM-18-05-02 (2005).
23. Greenwood, N., Earnshaw, A.: Chemistry of the Elements. Elsevier (2012).
24. Barin, I.: Thermodynamic Functions and Relations. Thermochem. Data Pure Subst., Wiley-VCH Verlag GmbH, p. 1 (1995).
25. Keller, E., Krämer, V.: A strong deviation from Vegard's Rule: X-ray powder investigations of the three quasi-binary phase systems $BiOX–BiOY$ (X, Y = Cl, Br, I). Z. Naturforsch. **60b**, 1255 (2005).
26. Gillberg, M.: Perite, a new oxyhalide mineral from Langban, Sweden. Ark. Miner. Geol. **2**, 565 (1960).
27. Ketterer, J., Krämer, V.: Structural characterization of the synthetic perites $PbBiO_2X$, X = I, Br, Cl. Mater. Res. Bull. **20**, 1031 (1985).